Pergamon

Chemical Engineering Science, Vol. 52, No. 15, pp. 2471–2482, 1997

Printed in Great Britain
PII: S0009-2509(97)00066-3
0009-2509/97 $17.00 + 0.00

Circulating fluidized-bed reactors

Daizo Kunii* and Octave Levenspiel†‡

*1-25-16 Nakamachi, Meguro ku, Tokyo 153, Japan; †Chemical Engineering Department, Oregon State University, Corvallis, OR, U.S.A.

(Accepted 15 May 1996)

Abstract—This paper develops a flow and contacting model to represent a CFB. Best estimates of contacting efficiencies are presented for the turbulent, fast fluidized, and pneumatic transport regimes of the CFB. Material balances are presented, ending up with conversion equations for first-order solid-catalyzed gas-phase reactions. Four examples show how to use this model and show its predictions. © 1997 Elsevier Science Ltd

Keywords: CFB reactors; conversion; circulating solids reactors.

1. INTRODUCTION

Let us first sketch the contacting regimes encountered when a bed of solids is fluidized by gas at progressively higher velocities. Because contacting differs in these contacting regimes, different reactor models must be used for predicting reactor behavior; see Fig. 1.

This paper deals with circulating solids reactors. These contain very fine particles which are fluidized at a rather high gas velocity, are blown out of the bed and reactor, and have to be replaced by fresh solids. We call these circulating fluidized beds (CFB).

We must first find what contacting regime is involved, and then deal with the reactor and its conversion equations.

2. CHARACTERIZATION OF PARTICLES

The equivalent spherical particle diameter is defined as

$$d_{\text{sph}} = \left(\begin{array}{l} \text{diameter of a sphere} \\ \text{which has the same} \\ \text{volume as the particle, } V \end{array} \right) = \left(\frac{6V}{\pi} \right)^{1/3} \quad (1)$$

and the particle sphericity ϕ_s is defined as

$$\phi_s = \left(\frac{\text{surface of a sphere}}{\text{surface of particle}} \right)_{\text{same volume}} . \quad (2)$$

From the above two expressions we define the particle size to be used for suspended solid reactors as

$$d_p = \phi_s d_{\text{sph}} . \quad (3)$$

For fine particles we evaluate the size by screen analysis, which gives d_{scr}. Unfortunately, there is no general relationship between d_{scr} and d_p. The best we can say for pressure drop considerations is

$$d_p \cong \begin{cases} \phi_s d_{\text{scr}} & \text{for irregular particles with no seeming longer or shorter dimension} \quad (4) \\ d_{\text{scr}} & \text{for irregular particles with one somewhat longer dimension but with length ratio not greater than 2:1 (eggs, for example)} \quad (5) \\ \phi_s^2 d_{\text{scr}} & \text{for irregular particles with one shorter dimension but with length ratio not less than 1:2 (pillows, for example)} \quad (6) \end{cases}$$

3. GAS/SOLID CONTACTING REGIMES

For given particles (d_p and ρ_s) and given superficial gas velocity through the bed (u_0), we first need to find what contacting regime is involved—packed bed, bubbling fluidized bed (BFB), or circulating fluidized bed (CFB), with its subregimes—turbulent fluidized, fast fluidized, or pneumatic transport. To do this first evaluate the dimensionless measures of particle size and gas velocity. These are defined as

$$d_p^* = d_p \left[\frac{\rho_g(\rho_s - \rho_g)g}{\mu^2} \right]^{1/3} \quad (7)$$

$$u^* = u \left[\frac{\rho_g^2}{\mu(\rho_s - \rho_g)g} \right]^{1/3} . \quad (8)$$

3.1. *Minimum fluidizing velocity*

The solids will be suspended when the pressure drop exceeds the weight of solids. This happens when the gas velocity exceeds the minimum fluidizing velocity. This velocity is given by Ergun (1952), and in

‡Corresponding author.

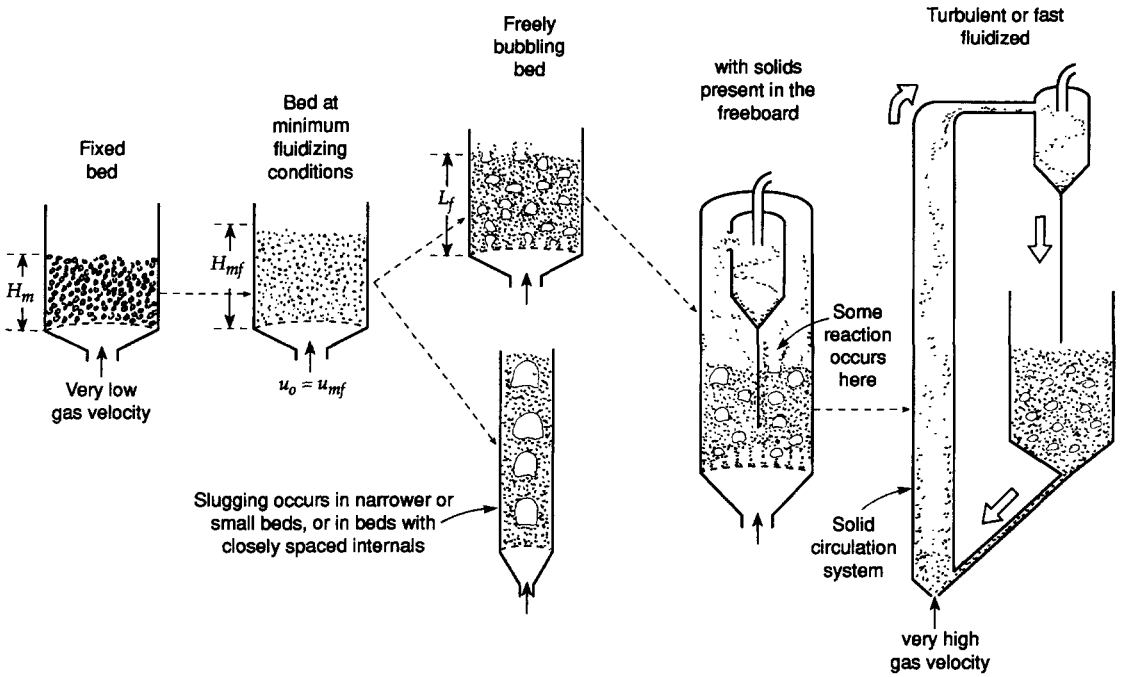

Fig. 1. Gas/solid contacting regimes depend on the gas velocity and bed geometry.

dimensionless form is

$$\frac{150(1-\varepsilon_{mf})}{\varepsilon_{mf}^3}u_{mf}^* + \frac{1.75}{\varepsilon_{mf}^3}(u_{mf}^*)^2 d_p^* = (d_p^*)^2 \qquad (9)$$

3.2. *Terminal velocity*, u_t

Individual particles are blown out of the bed when the gas velocity exceeds what is called the terminal velocity, u_t. Haider and Levenspiel (1989) give this velocity for spherical particles as

$$u_t^* = \left[\frac{18}{(d_p^*)^2} + \frac{0.591}{(d_p^*)^{1/2}}\right]^{-1} \qquad (10)$$

and for irregularly shaped particles of sphericity ϕ_s,

$$u_t^* = \left[\frac{18}{(d_p^*)^2} + \frac{2.335 - 1.744\phi_s}{(d_p^*)^{1/2}}\right]^{-1}. \qquad (11)$$

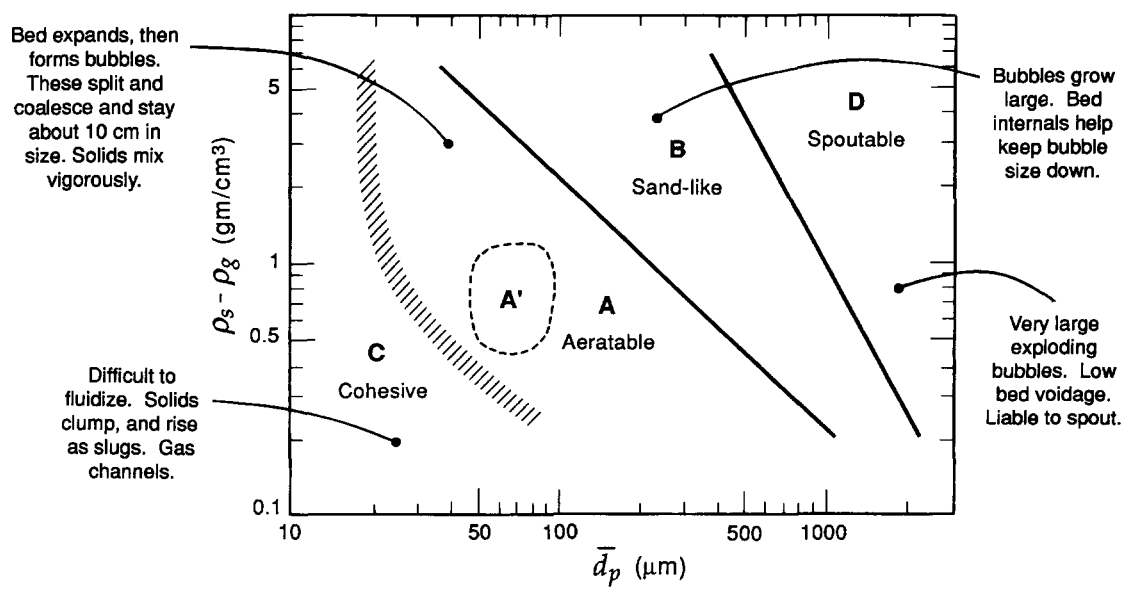

Fig. 2. Classification of solids in terms of their behavior when suspended by gas.

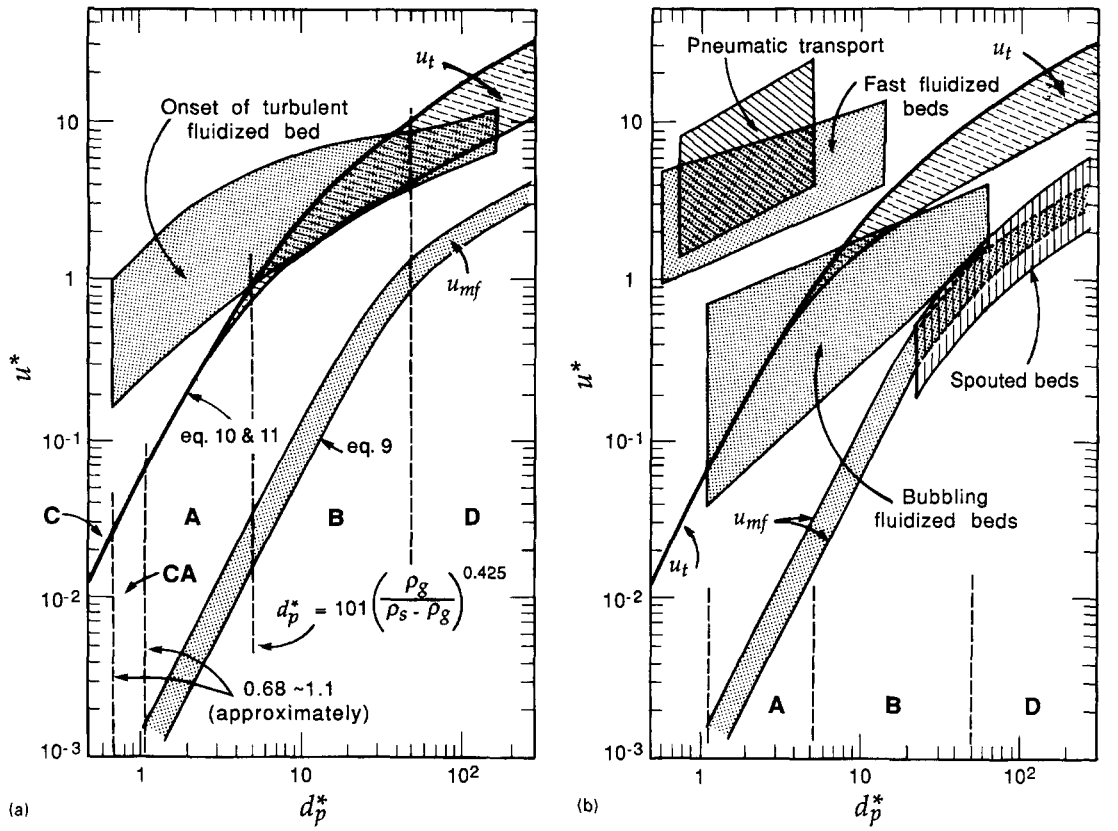

Fig. 3. The generalized map of gas/solid contacting.

3.3. *Behavior of suspended solids*

Based on observations of many different solids, Geldart (1973) and Geldart and Abrahamson (1978) came up with the A, B, C, D classification of solids, as shown in Fig. 2. BFB reactors usually use Geldart A, AB, and B solids. CFB reactors can go down to Geldart C solids.

3.4. *Gas–solid contacting regimes*

Grace (1986) prepared a graph to show the expected behavior of gas–solid systems all the way from BFB to CFB. Figure 3 show a somewhat modified version of his chart.

4. REACTORS WITH THROUGHFLOW OF SOLIDS, $u_0 > u_t$

4.1. *Observed behavior*

Very fine solids have a very small terminal velocity in gas, say mm/s, so with a reasonable throughflow of gas, say in m/s, solids are continuously carried out of the bed and have to be replaced with make-up solids. Let this throughflow be at a bed mass velocity of G_s (kg/m^{2}s). This leads to suspended solids reactors of various types depending on the ratio of u_t to u_0. Roughly, the solids distribution in the vessel is as shown in Fig. 4.

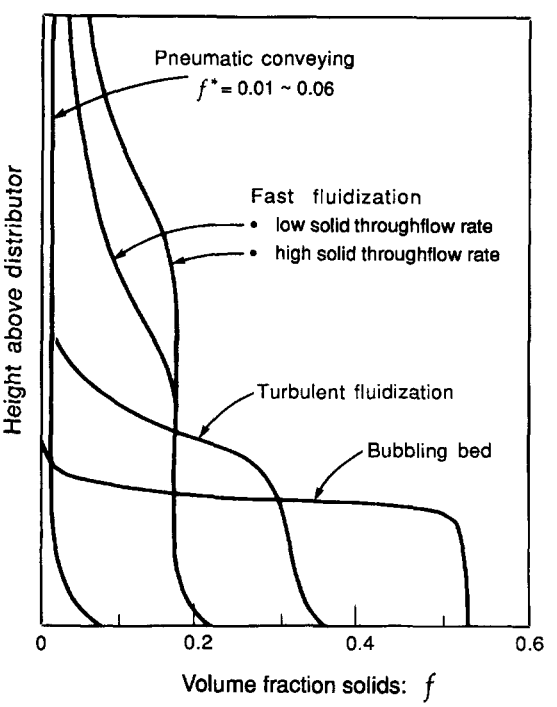

Fig. 4. Vertical distribution of solids in different contacting regimes.

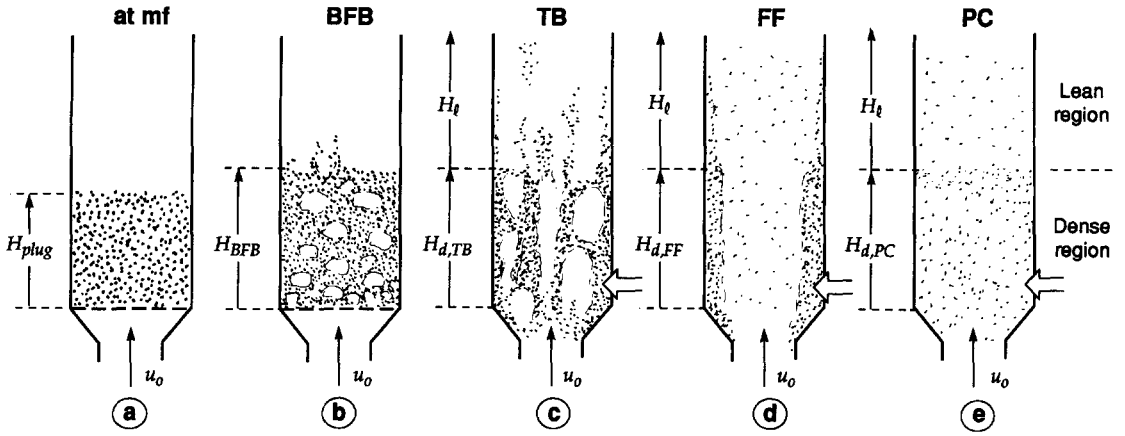

Fig. 5. Contacting models of vessels with throughflow of solids.

As observed, when the gas velocity of a bubbling fluidized bed (BFB) is progressively raised, the bubbling action becomes very violent, bubbles coalesce and become very large and finally expand to form a core space in the dense region of the vessel. At the same time the cloud and emulsion merge and retreat to the walls of the vessel. In this state we have a fast fluidized contactor (FF). Between the BFB and the FF regimes we have a difficult to describe turbulent bed (TB).

At even higher velocities the wall region thins, dissolves, as the vessel enters the pneumatic conveying regime (PC).

4.2. *Contacting models*

In CFB, solids are found throughout the vessels, in a dense region in the lower part of the vessel, and having a solid fraction f_d, and a lean region above, having a solid fraction f_l which decreases with height as shown in Fig. 5.

In the lower dense region of the vessel the fraction of solids is found to be

$$\begin{aligned} &\text{bubbling bed} && f_d = 0.4 \sim 0.6 \\ &\text{turbulent bed} && f_d = 0.2 \sim 0.4 \\ &\text{fast fluidized bed} && f_d = 0.06 \sim 0.2 \\ &\text{pneumatic transport} && f_d = 0.01 \sim 0.06\,. \end{aligned} \tag{12}$$

We visualize the *upper lean region* to consist of three phases:

- upflowing clumps of denser material of mean density ρ_2 rising at velocity u_2,
- downflowing clumps of mean density ρ_3 and solids sliding down the wall at u_3,
- lean mixture with dispersed solids of mean density ρ_1 rising at u_1.

This model also includes

- interchange rates between clumps and lean mixture at K_1,
- direction change from up to down at rate K_2.

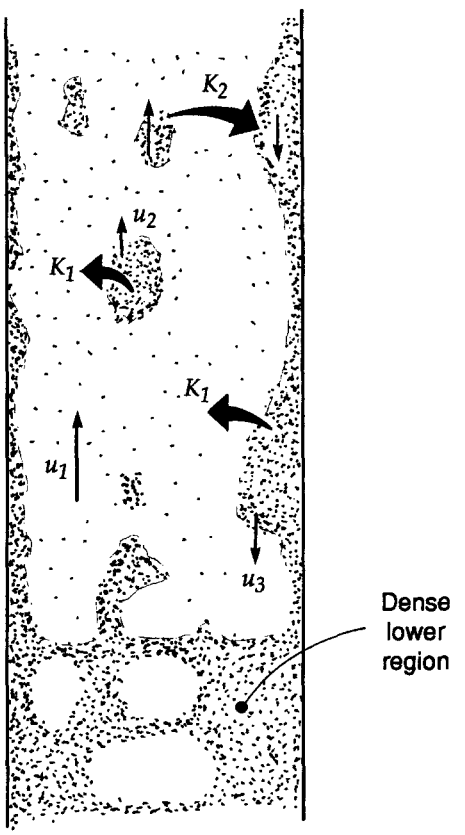

Fig. 6. Mechanism which yields the exponential decay of solids with height.

Figure 6 sketches the model. The differential equations representing this model are

$$G_s = G_{s1} + G_{s2} + G_{s3} = u_1\rho_1 + u_2\rho_2 - u_3\rho_3$$

$$\frac{d\rho_1}{dt} = u_1\frac{d\rho_1}{dz_\ell} = K_1(\rho_2 + \rho_3)$$

$$-u_2\frac{d\rho_2}{dz_\ell} = (K_1 + K_2)\rho_2$$

$$-u_3\frac{d\rho_3}{dz_\ell} = K_2\rho_2 - K_1\rho_3\,.$$

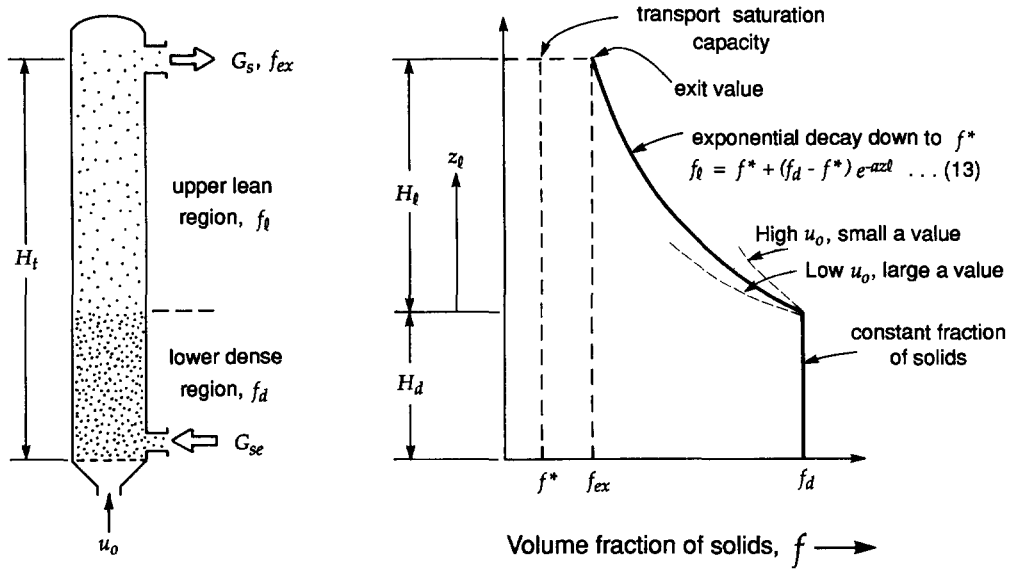

Fig. 7. The exponential decay model accounts for the distribution of solids in the vessel when the solids are in throughflow.

Solving these equations Kunii and Levenspiel (1991, p. 184) show the following.

- In a very tall (infinitely high) column the solid fraction falls exponentially from f_d to a lower limiting value f^*. The value f^* represents the *transport carrying capacity* of the gas, meaning that all the clumps of denser mixture have 'dissolved' into the flowing gas.
- In a shorter column the exiting solid fraction f_{ex} is greater than the limiting f^*.

We show this model in Fig. 7.

This distribution of solids is calculated from the model, and does approximate what is observed. So we retain this model.

4.3. *Material balance*

We picture the CFB (in particular the FF contactor) as shown in Figs 5(d) and 7, having a one zone upper lean region with a solids fraction f_l which decreases with height. The lower dense region having a constant solids fraction f_d consists of two zones, a lean core zone having solids f_{core}, and a dense wall zone having solids f_{wall}.

From experiments reported in the literature [15 studies for eq. (15) and 38 studies for eqs (16) and (17)], our best estimates today (see Kunii and Levenspiel, 1991, 1995) for needed physical quantities and relationships are

$$au_0 = \begin{cases} 2\text{–}4\ \text{s}^{-1} & \text{for Geldart A solids} \\ 5\ \text{s}^{-1} & \text{for Geldart AB solids} \\ 7\ \text{s}^{-1} & \text{for Geldart B solids} \end{cases} \quad (15)$$

f^* is independent of u_0

$\leqslant 0.02$ for Geldart A solids (16)

$\leqslant 0.01$ for Geldart B solids

f_d decreases with u_0 increases with d_p given by eq. (12)

and for the lower dense region,

$$f_{\text{core}} \cong f^* \quad (17)$$

$$f_{\text{wall}} = (1 - \varepsilon_{\text{wall}})(1 - \delta). \quad (18)$$

Lean region. Since $f_{\text{ex}} \ll 1$ the solid fraction in the exit stream is

$$f_{\text{ex}} \cong \frac{G_s}{\rho_s(u_0 - u_t)}. \quad (19)$$

Equation (14), written for the exit location, gives

$$f_{\text{ex}} = f^* + (f_d - f^*)\exp(-aH_l). \quad (20)$$

So the height of the lean region is

$$H_l = \frac{1}{a}\ln\left(\frac{f_d - f^*}{f_{\text{ex}} - f^*}\right). \quad (21)$$

The height of the dense region is then

$$H_d = H_t - H_l. \quad (22)$$

At any point in the lean region the fraction of solids is

$$f_l = f^* + (f_d - f^*)\exp(-az_l). \quad (14) \text{ or } (23)$$

This gives the mean fraction of solids in the lean region to be

$$\bar{f}_l = \frac{1}{H_l}\int_0^{H_l} f_l\,\mathrm{d}z_l = f^* + \frac{f_d - f_{\text{ex}}}{aH_l} \quad (24)$$

and the mean solid fraction in the vessel as a whole is

$$\bar{f}_{\text{vessel}} = \frac{\bar{f}_l H_l + f_d H_d}{H_t} \tag{25}$$

So the weight of catalyst in these regions is

$$\begin{aligned} W_l &= A_t \rho_s H_l \bar{f}_l \\ W_d &= A_t \rho_s H_d f_d \\ W_t &= W_l + W_d. \end{aligned} \tag{26}$$

These equations relate u_0, G_s, and W. Thus, if you are given a specific gas velocity and you want a specific weight of solids in the reactor, these equations will tell you what solid feed rate to use.

5. PERFORMANCE AND CONTACT EFFICIENCY OF CFB REACTORS

Consider a first-order solid-catalyzed reaction

$$A \to R, \quad -r'''_A = k'''C_A \quad \text{or} \quad -r'_A = k'C_A. \tag{27}$$

In Fig. 8 let us sketch the contacting as viewed by our proposed reactor models for the various contacting regimes.

5.1. *Bed at minimum fluidization*

For a bed at minimum fluidization we assume plug flow [see Fig. 8(a)]. We then write for any level in the reactor

$$-u_0 \frac{dC_A}{dz} = f_{\text{plug}} \eta_{\text{plug}} k''' C_A. \tag{28}$$

But for plug flow $\eta_{\text{plug}} = 1$, integration gives

$$\ln \frac{C_{A0}}{C_{Ad}} = \frac{f_{\text{plug}} k''' H_{\text{plug}}}{u_0} = \frac{k' W_t}{u_0 A_t}. \tag{29}$$

5.2. *Bubbling fluidized bed*

For a bubbling fluidized bed with its three connected zones [see Fig. 8(b)], we assume bubble upflow but no flow through clouds and emulsion, only interchange K_{bc} and K_{ce}. So, as shown by Kunii and Levenspiel (1991, p. 291), the integrated conversion expression is

$$\ln \frac{C_{A0}}{C_{Aex}} = \left[f_b k''' + \frac{1}{\dfrac{1}{\delta_{\text{BFB}} K_{bc}} + \dfrac{1}{f_c k''' + \dfrac{1}{(1/\delta_{\text{BFB}} K_{ce}) + 1/f_e k'''}}} \right] \times \frac{H_{\text{BFB}}}{u_0}. \tag{30}$$

For a dense bed of height H_{BFB} and containing the same amount of solids but with solids uniformly distributed throughout, and with plug flow of gas, we have

$$\ln \frac{C_{A0}}{C_{Aex}} = \frac{(f_b + f_c + f_e) k''' H_{\text{BFB}}}{u_0} \eta_{\text{BFB}}. \tag{31}$$

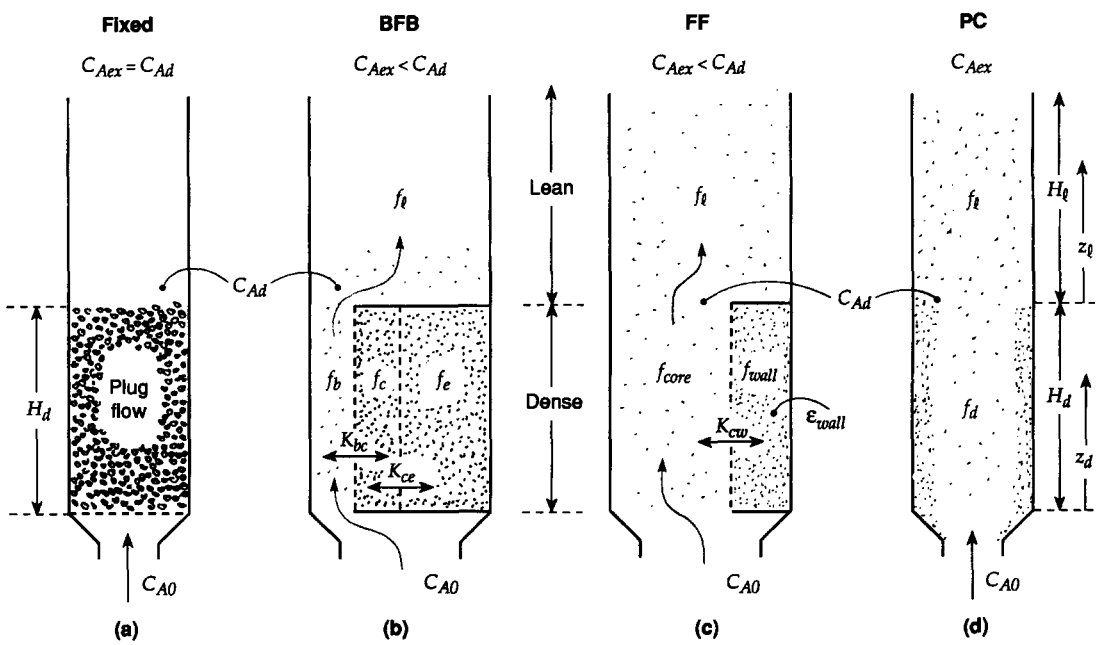

Fig. 8. Proposed reactor models for the various contacting regimes.

The contacting efficiency is then given by eq. (30) divided by eq. (31), or

$$\eta_{BFB} = \frac{\left[f_b + \dfrac{1}{\dfrac{k'''}{\delta_{BFB} K_{bc}} + \dfrac{1}{f_c + \dfrac{1}{(k'''/\delta_{BFB} K_{ce} + 1/f_e)}}} \right]}{f_b + f_c + f_e}. \tag{32}$$

5.3. *Fast fluidization*

For fast fluidization we have distinctly different expressions for conversion in the upper lean and lower dense regions; see Fig. 8(c).

For the dense region the three zones of a BFB collapse into two. Thus,

$$f_b \Rightarrow f_{core}, \quad f_c + f_e \Rightarrow f_{wall}, \quad K_{ce} \Rightarrow \infty \text{ and } K_{bc} \Rightarrow K_{cw}.$$

So the performance expression of the BFB reduces, for the dense region of FF reactors, to

$$\ln \frac{C_{A0}}{C_{Ad}} = \left[f_{core} k''' + \frac{1}{(1/\delta_{d,FF} K_{cw}) + 1/f_{wall} k'''} \right] \frac{H_{d,FF}}{u_0}. \tag{33}$$

The various constants appearing in this expression are not well known today; however, we estimate them as follows:

$$\begin{aligned} f_{core} &\cong f^* \cong 0.01 \\ \delta_{d,FF} &= 0.6\text{–}0.9 \\ K_{cw} &= 5\text{–}20\ s^{-1} \\ \varepsilon_{wall} &\cong \varepsilon_{mf} \cong 0.5\text{–}0.6. \end{aligned} \tag{34}$$

The contact efficiency compared to plug flow, by an argument similar to the BFB, is

$$\eta_{d,FF} = \frac{\left[f_{core} + \dfrac{1}{(k'''/\delta_{d,FF} K_{cw}) + 1/f_{wall}} \right]}{f_{core} + f_{wall}}. \tag{35}$$

For the lean region of the FF reactor of height H_l and with decreasing solid fraction with height, the rate of any level is

$$-u_0 \frac{dC_A}{dz} = \eta_l f_l k''' C_A. \tag{36}$$

The term f_l is given by eq. (23). The efficiency term for FF, TB, and above the BFB are not well known today. The only studies to date (Furusaki *et al.*, 1976; see also Kunii and Levenspiel, 1991, p. 283) show that the contacting efficiency in the lean phase can be represented by an exponential expression

$$\eta_l = 1 - (1 - \eta_d) e^{-bz_l} \tag{37}$$

where $b = 6.62\ m^{-1}$, by experiment. This expression shows that the lean region efficiency rises exponentially from η_d at $z_l = 0$ to $\eta_l = 1$ very high up in the bed. With f_l and η_l replaced by eqs (23) and (37), integration of eq. (36) gives

$$\begin{aligned} \ln \frac{C_{Ad}}{C_{Aex}} = {} & \frac{k''' f^*}{u_0} \left[H_l - \frac{1 - \eta_d}{b} (1 - e^{-bH_l}) \right] \\ & + \frac{k'''(f_d - f^*)}{u_0} \left[\frac{1 - e^{-aH_l}}{a} \right. \\ & \left. - \frac{1 - \eta_d}{a + b} (1 - e^{-(a+b)H_l}) \right] \end{aligned} \tag{38}$$

and for the special case where $\eta_d = 1$ (very lean solids, high gas velocity, pneumatic flow)

$$\ln \frac{C_{Ad}}{C_{Aex}} = \frac{k''' f^* H_l}{u_0} + \frac{k'''(f_d - f^*)}{u_0 a} (1 - e^{-aH_l}). \tag{39}$$

Finally, the overall conversion is given by eq. (38) or (39) with eq. (33):

$$\frac{C_{Aex}}{C_{A0}} = \frac{C_{Aex}}{C_{Ad}} \cdot \frac{C_{Ad}}{C_{A0}} \quad \text{and} \quad X_{A\,overall} = 1 - \frac{C_{Aex}}{C_{A0}}. \tag{40}$$

For pneumatic conveying all the particles are evenly dispersed in the gas. This makes contacting ideal or close to ideal. So, if gas passes in plug flow up the reactor the contact efficiency

$$\eta_d = \eta_l = 1 \tag{41}$$

and the regular plug flow expression, eq. (29), applies:

$$\ln \frac{C_{A0}}{C_{Aex}} = \frac{(f_d H_d + \bar{f}_l H_l) k'''}{u_0}. \tag{42}$$

The reliability of the above conversion predictions all depend on the reasonableness of the models and on the values of the parameters chosen.

$$f^* \quad \delta \quad a \quad b.$$

Finally, probably the most important value of models such as presented here is to be a guide for experimenters, and to suggest areas where research is needed.

6. DESIGN PROBLEMS

To illustrate the use of the material presented here, consider a particular process requirement and let us explore various design alternatives to meet this requirement. For this let us suppose that we want to find the fractional conversion of A to R. We are told that our catalyst is very active with first-order kinetics:

$$A \rightarrow R, \quad -\frac{1}{W} \frac{dN_A}{dt} = k' C_A,$$

$$\begin{cases} k' = 0.01\ m^3/kg\ cat\ s \\ k''' = 10\ m^3/m^3\ cat\ s. \end{cases}$$

Figure 9 shows the four design alternatives that we will consider. We refer to this figure as we proceed.

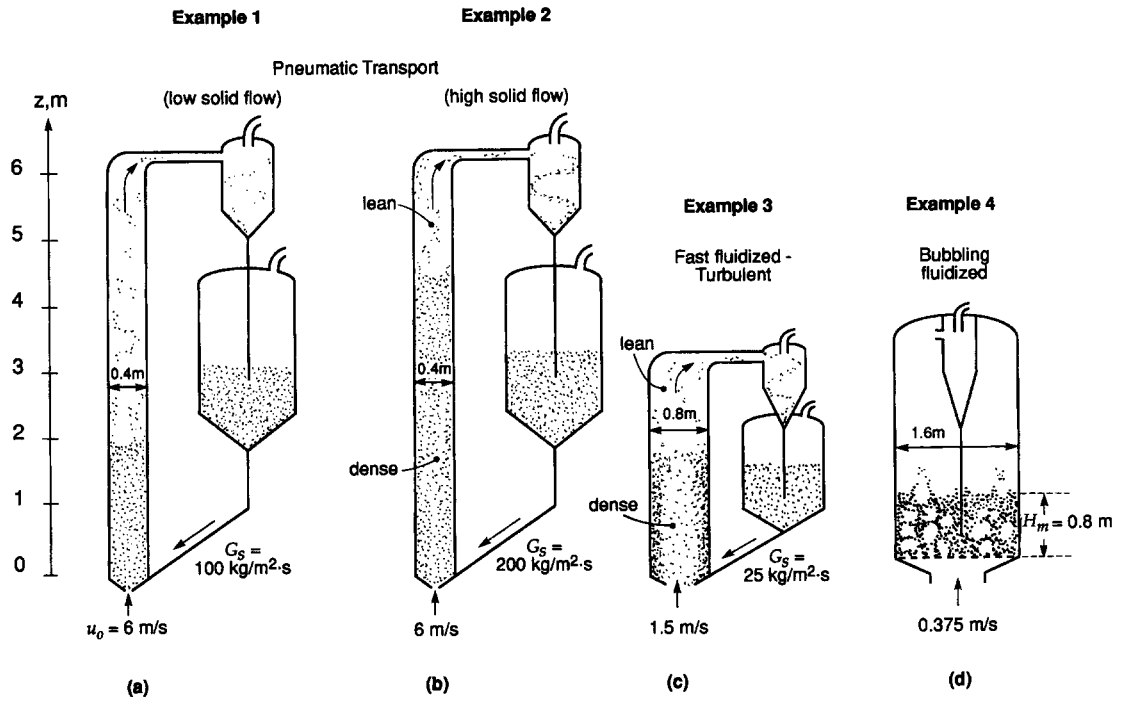

Fig. 9. Four design alternatives for reactors treating a given flow rate of reactant gas.

Data. We want to treat $\dot{n} = 40$ mol/s of pure A feed at 300 K and 1.3 atm under which condition the properties of gas and solid (porous catalyst particles) are

$$\text{Gas} \begin{cases} \dot{n} = 40 \text{ mol/s} \\ \rho_g = 1.2 \text{ kg/m}^3 \\ \mu = 1.8 \times 10^{-5} \text{ kg/m s} \\ D = 4 \times 10^{-5} \text{ m}^2/\text{s} \quad \text{in the bed} \end{cases}$$

$$\text{Porous catlyst solid:} \begin{cases} \text{shape is spherical} \\ \rho_s = 1000 \text{ kg/(m cat)}^3 \\ D_{\text{eff}} = 10^{-7} \text{ m}^3/\text{m cat s}, \\ \qquad \text{in the porous particle.} \end{cases}$$

From this data the volumetric flow rate of feed gas is

$$v_0 = u_0 A = \frac{\dot{n}RT}{p} = \frac{40(8.314)300}{1.3(101\,325)} = 0.7574 \text{ m}^3/\text{s}.$$

6.1. *Example 1. Pneumatic transport reactor*

Because the catalyst is said to be very active, let us choose very fine particles, $d_p = 55$ μm, and a vessel diameter of $d_t = 0.4$ m. The superficial gas velocity for this vessel is then

$$u_0 = \frac{v_0}{A} = \frac{0.7574}{\frac{1}{4}\pi(0.4)^2} = 6.0 \text{ m/s}.$$

This high gas velocity and small particle size suggests that solids may be rapidly carried out of the reactor, so we may need to use solid circulation. So let us tentatively choose a solid circulation system with a reactor of height $H_t = 6$ m and with a solid circulation rate of $G_s = 100$ kg/m² s. This design is shown as Fig. 9(a).

Solution:

(1) From Fig. 2 we see that we have here a Geldart A solid.

(2) From eqs (7) and (8)

$$d_p^* = d_p \left[\frac{\rho_g(\rho_s - \rho_g)g}{\mu^2} \right]^{1/3}$$

$$= 55 \times 10^{-6} \left[\frac{1.2(1000 - 1.2)9.8}{(1.8 \times 10^{-5})^2} \right]^{1/3}$$

$$= 1.82$$

$$u_0^* = u_0 \left[\frac{\rho_g^2}{\mu(\rho_s - \rho_g)g} \right]^{1/3}$$

$$= 6 \left[\frac{(1.2)^2}{1.8 \times 10^{-5}(1000 - 1.2)9.8} \right]^{1/3}$$

$$= 12.08.$$

(3) The terminal velocity, from eqs (10) and (8),

$$u_t^* = \left[\frac{18}{(d_p^*)^2} + \frac{0.591}{(d_p^*)^{1/2}}\right]^{-1} = 0.1703$$

$$u_t = u_t^* \left[\frac{\mu(\rho_s - \rho_g)g}{\rho_g^2}\right]^{1/3}$$

$$= 0.1703 \left[\frac{1.8 \times 10^{-5}(1000 - 1.2)9.8}{(1.2)^2}\right]^{1/3}$$

$$= 0.084545 \text{ m/s}.$$

This says that at 8 cm/s solids are blown out of the bed. Note, we plan to use a velocity of 6 m/s.

(4) Figure 3 shows that we are in the *Pneumatic transport* regime, so we guessed right when we chose the vessel of Fig. 9(a).

(5) Evaluate the constants, from eqs (12), (15) and (16):

$$f_d = 0.06$$
$$f^* = 0.01$$
$$u_0 a = 3 \text{ s}^{-1} \quad \text{or} \quad a = 0.5 \text{ m}^{-1}.$$

(6) From eq. (19)

$$f_{ex} = \frac{G_s}{\rho_s(u_0 - u_t)} = \frac{100}{1000(6 - 0.084545)}$$

$$= 0.0169.$$

(7) Locate the dense and lean regions, from eq. (21),

$$H_l = \frac{1}{a} \ln\left(\frac{f_d - f^*}{f_{ex} - f^*}\right)$$

$$= \frac{1}{0.5} \ln\left(\frac{0.06 - 0.01}{0.0169 - 0.01}\right) = 3.9610 \text{ m}$$

$$H_d = 6 - 3.9610 = 2.0390 \text{ m}.$$

(8) Find $\bar{f}_l$ in the lean region, from eq. (24),

$$\bar{f}_l = f^* + \frac{f_d - f_{ex}}{aH_l} = 0.01 + \frac{0.06 - 0.0169}{0.5(3.9610)}$$

$$= 0.0318.$$

(9) The weight of catalyst in the vessel, from eq. (26),

$$W_d = A_t \rho_s H_d f_d$$

$$= \frac{\pi}{4}(0.4)^2(1000)(2.0390)(0.06)$$

$$= 15.3737 \text{ kg}$$

$$W_l = A_t \rho_s H_l \bar{f}_l$$

$$= \frac{\pi}{4}(0.4)^2(1000)(3.9610)(0.0318)$$

$$= 15.8286 \text{ kg}$$

Therefore $W_{total} = 31.2$ kg.

(10) Estimate the contact efficiencies in the two regimes:
- For the dense region, from eq. (41), $\eta_d = 1$.
- For the lean region, from eq. (41), $\eta_l = 1$.

(11) Since we have plug flow in both regions we can use eq. (42) instead of eq. (33) for the dense region and eq. (38) for the lean region. Incidentally, you would get the same answer with these more complicated equations. Thus, we have

$$\ln \frac{C_{A0}}{C_{Aex}}$$

$$= \frac{[(0.06)(2.0390) + (0.0318)(3.9610)]10}{6}$$

$$= 0.4138.$$

Therefore,

$$\frac{C_{Aex}}{C_{A0}} = 0.6611 \quad \text{or} \quad X_{A,\text{total}} = 34\%.$$

6.2. *Example 2. Pneumatic transport reactor*

The design of Example 1 is unacceptable because conversion is too low. Let us see if we can raise it by doubling the solid throughflow rate to $G_s = 200 \text{ kg/m}^2\text{s}$ while keeping all else unchanged; see Fig. 9(b).

Solution: Following the procedure of Example 1 we find

- pneumatic transport with $\eta = 1$,
- $H_d = 4.5$ m, instead of 2.0 m,
- $W_{total} = 42.50$ kg, instead of 31.20 kg.

so

$$X_{A,\text{overall}} = 42\%.$$

This is better than that found in Example 1 but still not good enough. So let us try still other alternatives.

6.3. *Example 3. Turbulent or fast fluidized reactor*

Maybe the chosen gas velocity was too high in Examples 1 and 2. Let us try a lower gas velocity, $u_0 = 1.5$ m/s, in a squatter vessel, $d_t = 0.8$ m and $H_t = 3$ m, while keeping the throughflow rates of gas and solids unchanged from Example 1; see Fig. 9(c). Also take

$$f_d = 0.16 \frac{\text{m}^3 \text{ of solids in the lower dense region}}{\text{m}^3 \text{ of dense region}}$$

$$f^* = 0.01 \frac{\text{m}^3 \text{ of solids}}{\text{m}^3 \text{ of vessel}}, \quad \text{during pneumatic conveying}$$

$$\delta = 0.7 \frac{\text{m}^3 \text{ of core}}{\text{m}^3 \text{ of dense region}}$$

$$K_{cw} = 5 \text{ s}^{-1}.$$

Solution: Following the procedures of Example 1 we find

- we have a turbulent or fast fluidized bed with $\eta_d = 0.72$,
- $H_d = 1.5$ m,
- $W_{\text{total}} = 165$ kg,

so

$$X_{A,\text{overall}} = 82\%.$$

6.4. *Example 4. Bubbling fluidized reactor*

It just occurred to us that we may have chosen particles smaller than was needed in Examples 1–3. We should have checked for this with the Thiele modulus, but did not. Let us do this now. What we find, see Levenspiel (1996b), is

$$M_T = \frac{d_p}{6}\sqrt{\frac{k'''}{D_{\text{eff}}}} = \frac{55\times10^{-6}}{6}\sqrt{\frac{10}{10^{-7}}} = 0.092.$$

This is a much smaller Thiele modulus than needed, so we can safely use larger particles. Let us try $d_p = 220\times10^{-6}$ m. For these the Thiele modulus is

$$M_T = \frac{220\times10^{-6}}{6}\sqrt{\frac{10}{10^{-7}}} = 0.366.$$

This size of solid is still free from internal resistance to diffusion. So let us adopt these solids and again double the bed diameter and lower the gas velocity accordingly so as to keep the gas flow unchanged; see Fig. 9(d).

Calculate the conversion for these conditions.

Solution: We first find that we are right in the middle of the BFB regime with negligible carryover of solids, $u_0 < u_t$. No throughflow of solids is needed, so let us use a BFB with the following properties:

$$d_t = 1.6\text{ m}, \quad d_b = 0.16\text{ m}, \quad \text{spherical particles}$$

$$H_{mf} = 0.8\text{ m}, \quad \alpha = 0.4, \quad d_p = 220\times10^{-6}\text{ m}$$

$$\varepsilon_{mf} = 0.6, \quad f_b = 0.003, \quad u_0 = 0.375\text{ m/s}.$$

In the fluidized bed $D = 4\times10^{-5}$ m^3/m cat s.

For this system we find, by the methods outlined in Levenspiel (1996a),

$$W_t = 643\text{ kg} \quad \text{with} \quad \eta = 11\%$$

so

$$X_{A,\text{overall}} = 61\%.$$

6.5. *Comments about these four examples*

We have explored various design alternatives and we have shown how to determine the performance expected for each, as summarized in Fig. 10.

Some designs give very low conversions, others high. Some suspend a large inventory of solids (643 kg

Example number	W,kg	Contact efficiency	Conversion X_A
1	31	$\eta = 1.00$	34%
2	42	$\eta = 1.00$	43%
3	165	$\eta_d = 0.72$	82%
4	643	$\eta = 0.11$	61%

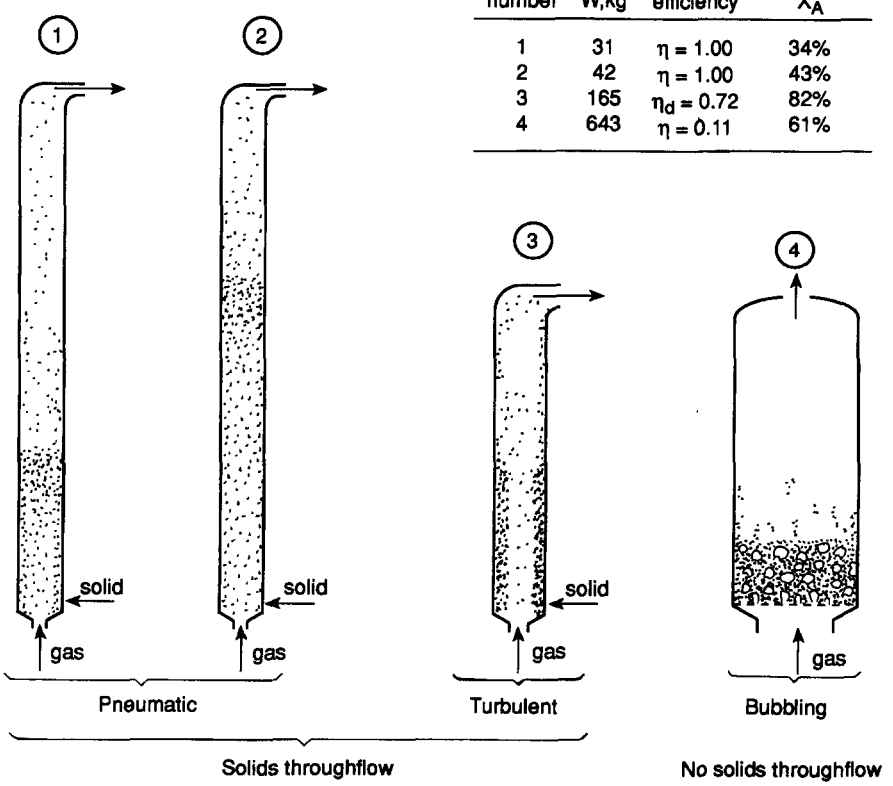

Fig. 10. A wide range of conversions result from the four design alternatives. Fast fluidization turns out to be best.

in Example 4), others a small inventory (31 kg in Example 1). Consequently, the pressure drop and pumping requirement can differ greatly for these designs.

Although the BFB has a very low contacting efficiency (11%), the amount of solid used there is so much greater than in the very much leaner solid throughflow systems (see Examples 1–3); hence, the intermediate conversion in the bubbling fluidized bed.

In these examples the FF turns out best, however the conclusions found here hold only for the conditions examined in the above examples. In other situations the advantage may be with a different contacting regime. So, in all cases it would be wise to examine a wide range of possible operating conditions and particle sizes.

Finally, we should point out that we have only presented what may be called '$10 solutions' here. Certainly, one can build on this approach.

NOTATION

a	decay constant for solid fraction in the lean region of a CFB; see Fig. 6, m^{-1}
A_t	cross-sectional area of a CFB reactor, m^2
b	decay constant for gas/solid contact inefficiency in the lean region of a CFB; see eq. (23), m^{-1}
BFB	bubbling fluidized bed
C_A	concentration of reactant A, mol/m^3
CFB	circulating fluidized bed
d_p, d_{scr}, d_{sph}	measures of particle diameter; see eqs (1)–(6), m
d_p^*	dimensionless measure of particle diameter; see eq. (7)
D_{eff}	diffusion coefficient of gas in the porous catalyst, m^3 gas/m solid s
f_i, ($i = b, c, e, d, l$, etc.)	volume of solids in section i of a slice of bed/volume of that slice of bed, m^3 solid/m^3 reactor
f^*	solid fraction in gas stream in pneumatic conveying conditions
g	acceleration due to gravity ($= 9.8\ m/s^2$)
G_s	mass velocity of solids through the CFB, kg/m^2 of bed s
H_d, H_l, H_{total}	height of regions and of the CFB, m
k'	first-order reaction rate constant based on unit mass of catalyst solid, m^3 gas/kg cat s
k'''	first-order reaction rate constant based on unit volume of catalyst solid, m^3 gas/m^3 cat s
K_{bc}, K_{ce}, K_{be}	gas exchange coefficients between bubble, cloud, and emulsion, m^3 gas moving from one zone to the other/m^3 of bubbles s
K_{cw}	gas interchange coefficient between core and wall region m^3 gas moving from one zone to the other/m^3 of core s
K_1, K_2	interchange coefficients; see above eq. (13), s^{-1}
M_T	Thiele modulus, defined in Example 4, dimensionless
$\dot{n}$	molar feed rate, mol/s
r'_A	reaction rate based on mass of catalyst, mol/kg s
r'''_A	reaction rate based on volume of catalyst, mol/m^3 cat · s
u_0	superficial gas velocity in the reactor m^3/m^2 vessel s
u_t	terminal velocity of a particle falling through the gas, m/s
u^*	dimensionless gas velocity; see eq. (8)
v_0	volumetric feed rate, m^3/s
W	weight of catalyst, kg
X_A	fraction of reactant A converted, dimensionless
z	height in the lean region of a CFB, m

Greek letters

α	wake volume/bubble volume, dimensionless
δ	volume fraction of lean region, bubble or core, in a section of reactor, dimensionless
ε_{wall}	void fraction in the wall zone, dimensionless
μ	viscosity of gas, kg/m s
η	efficiency of reactor when compared to plug flow, kg/kg
ρ	density, kg/m^3
ϕ_s	sphericity of solid particles; see eq. (2), dimensionless

Subscripts

b	bubble
c	cloud
core	in the core region of a CFB
d	dense region of a FF contactor
f	fluidized condition
g	gas phase
l	lean region of a CFB
mf	at minimum fluidizing conditions
s	solid
wall	sliding down the wall of a CFB

REFERENCES

Ergun, S. (1952) Fluid flow through packed columns. *Chem. Engng Prog.* **48**, 89.

Furusaki, S., Kikuchi, T. and Miyauchi, T. (1976) Axial distribution of reactivity inside a fluid bed contactor. *A.I.Ch.E. J.* **22**, 354–361.

Geldart, D. (1973) Types of gas fluidization. *Powder Technol.* **7**, 285–292.

Geldart, D. and Abrahamsen, A. R. (1978) Homogeneous fluidization of fine powders using various gases and pressures. *Powder Technol.* **19**, 133–136.

Grace, J. R. (1986) Contacting modes and behavior classification of gas–solid and other two-phase suspensions. *Can. J. Chem. Engng* **64**, 353–363.

Haider, A. and Levenspiel, O. (1989) Drag coefficient and terminal velocity of spherical and nonspherical particles. *Powder Technol.* **58**, 63–70.

Kunii, D. and Levenspiel, O. (1991) *Fluidization Engineering*, 2nd Edn. Butterworth-Heinemann, Boston, MA, U.S.A.

Kunii, D. and Levenspiel, O. (1995) The vertical distribution of solids in circulating fluidized beds. In *Fluidization* VIII, Tours, pp. 17–24.

Levenspiel, O. (1996a) *The Chemical Reactor Omnibook*, Chap. 25. OSU Bookstores, Corvallis, OR, U.S.A.

Levenspiel, O. (1996b) *The Chemical Reactor Omnibook*, pp. 22.3 or 23.1. OSU Bookstores, Corvallis, OR, U.S.A.